This paper is published as part of a *PCCP* themed issue on chemical dynamics of large amplitude motion

Guest editors: David J. Nesbitt and Martin A. Suhm

Editorial

Chemical dynamics of large amplitude motion
David J. Nesbitt and Martin A. Suhm, Phys. Chem. Chem. Phys., 2010
DOI: 10.1039/c0cp90051f

Papers

The benefits of alternation and alkylation: large amplitude hydrogen bond librational modes of alcohol trimers and tetramers
R. Wugt Larsen and M. A. Suhm, *Phys. Chem. Chem. Phys*., 2010
DOI: 10.1039/b925578h

Analysis of the FASSST rotational spectrum of NCNCS in view of quantum monodromy
Brenda P. Winnewisser, Manfred Winnewisser, Ivan R. Medvedev, Frank C. De Lucia, Stephen C. Ross and Jacek Koput, *Phys. Chem. Chem. Phys*., 2010
DOI: 10.1039/b922023b

Ring-puckering motion in cyclopentene studied by time-resolved rotational coherence spectroscopy and *ab initio* calculations
Maksim Kunitski, Stefan Knippenberg, Maxim Gelin, Christoph Riehn, Andreas Dreuw and Bernhard Brutschy, *Phys. Chem. Chem. Phys.*, 2010
DOI: 10.1039/b925388b

Periodic bond breaking and making in the electronic ground state on a sub-picosecond timescale: OH bending spectroscopy of malonaldehyde in the frequency domain at low temperature
Nils O. B. Lüttschwager, Tobias N. Wassermann, Stéphane Coussan and Martin A. Suhm, *Phys. Chem. Chem. Phys*., 2010
DOI: 10.1039/c002345k

Large-amplitude vibrations of an N–H···π hydrogen bonded *cis*-amide–benzene complex
Chantal Pfaffen, Hans-Martin Frey, Philipp Ottiger, Samuel Leutwyler, Rafa A. Bachorz and Wim Klopper, *Phys. Chem. Chem. Phys*., 2010
DOI: 10.1039/c002056g

Vibration–rotation-tunneling states of the benzene dimer: an *ab initio* study
Ad van der Avoird, Rafa Podeszwa, Krzysztof Szalewicz, Claude Leforestier, Rob van Harrevelt, P. R. Bunker, Melanie Schnell, Gert von Helden and Gerard Meijer, *Phys. Chem. Chem. Phys*., 2010
DOI: 10.1039/c002653k

Dissociation of nitric acid at an aqueous surface: Large amplitude motions in the contact ion pair to solvent-separated ion pair conversion
Shuzhi Wang, Roberto Bianco and James T. Hynes, *Phys. Chem. Chem. Phys*., 2010
DOI: 10.1039/c002299n

Vibrational dynamics around the conical intersection: a study of methoxy vibrations on the ^2XE surface
Jayashree Nagesh and Edwin L. Sibert, *Phys. Chem. Chem. Phys*., 2010
DOI: 10.1039/c002593c

Rotational study of carbon monoxide isotopologues in small ^{4}He clusters
P. L. Raston, Y. Xu, W. Jäger, A. V. Potapov, L. A. Surin, B. S. Dumesh and S. Schlemmer, *Phys. Chem. Chem. Phys.*, 2010
DOI: 10.1039/c0cp00193g

Simulating ligand-induced conformational changes in proteins using a mechanical disassembly method
Juan Cortés, Duc Thanh Le, Romain Iehl and Thierry Siméon, *Phys. Chem. Chem. Phys*., 2010
DOI: 10.1039/c002811h

Molecular dynamic simulations of OH-stretching overtone induced photodissociation of fluorosulfonic and chlorosulfonic acid
Priyanka Gupta, Joseph R. Lane and Henrik G. Kjaergaard, *Phys. Chem. Chem. Phys*., 2010
DOI: 10.1039/c003073m

Vibrational specificity of proton-transfer dynamics in ground-state tropolone
Daniel Murdock, Lori A. Burns and Patrick H. Vaccaro, *Phys. Chem. Chem. Phys.,* 2010
DOI: 10.1039/c003140b

New insights into the photodynamics of acetylacetone: isomerization and fragmentation in low-temperature matrixes
A. Trivella, T. N. Wassermann, J. M. Mestdagh, C. Manca Tanner, F. Marinelli, P. Roubin and S. Coussan, *Phys. Chem. Chem. Phys*., 2010
DOI: 10.1039/c003593a

***Ab initio* anharmonic vibrational frequency predictions for linear proton-bound complexes OC–H^+–CO and N_2–H^+–N_2**
Kasia Terrill and David J. Nesbitt, *Phys. Chem. Chem. Phys*., 2010
DOI: 10.1039/c002774j

High resolution electronic spectroscopy of 4-methylanisole in the gas phase. Barrier height determinations for the methyl group torsional motion
Philip J. Morgan, Leonardo Alvarez-Valtierra and David W. Pratt, *Phys. Chem. Chem. Phys*., 2010
DOI: 10.1039/c000757a

Determination of precise relative energies of conformers of *n*-propanol by rotational spectroscopy
Zbigniew Kisiel, Orest Dorosh, Atsuko Maeda, Ivan R. Medvedev, Frank C. De Lucia, Eric Herbst, Brian J. Drouin, John C. Pearson and Steven T. Shipman, *Phys. Chem. Chem. Phys*., 2010
DOI: 10.1039/c002156c

Microwave spectroscopy of the Ne–OH($^2\Pi_j$) complex and three-dimensional intermolecular potentials
Yoshihiro Sumiyoshi, Ippei Funahara, Kazuya Sato, Yasuhiro Ohshima and Yasuki Endo, *Phys. Chem. Chem. Phys*., 2010
DOI: 10.1039/c002193h

Rotational spectra of *o*-, *m*-, and *p*-cyanophenol and internal rotation of *p*-cyanophenol
Andrew R. Conrad, Nathan Z. Barefoot and Michael J. Tubergen, *Phys. Chem. Chem. Phys*., 2010
DOI: 10.1039/c001705a

Hydrogen exchange in formic acid dimer: tunnelling above the barrier
David Luckhaus, Phys. Chem. Chem. Phys., 2010
DOI: 10.1039/c001253j

Tunneling dynamics and spectroscopic parameters of monodeuterated hydronium, H_2DO^+, from a combined analysis of infrared and sub-millimeter spectra
Holger S. P. Müller, Feng Dong, David J. Nesbitt, Takashi Furuya and Shuji Saito, *Phys. Chem. Chem. Phys*., 2010
DOI: 10.1039/c002067b

On the efficiency of treating singularities in triatomic variational vibrational computations. The vibrational states of H+3 up to dissociation
Tamás Szidarovszky, Attila G. Császár and Gábor Czakó, *Phys. Chem. Chem. Phys*., 2010
DOI: 10.1039/c001124j

Theoretical rotation–torsion spectra of HSOH
Andrey Yachmenev, Sergei N. Yurchenko, Per Jensen, Oliver Baum, Thomas F. Giesen and Walter Thiel, *Phys. Chem. Chem. Phys*., 2010
DOI: 10.1039/c002803g

Chirality of and gear motion in isopropyl methyl sulfide: A Fourier transform microwave study
Eizi Hirota, Keisuke Sakieda and Yoshiyuki Kawashima, *Phys. Chem. Chem. Phys*., 2010
DOI: 10.1039/c002314k

Torsional energy levels of nitric acid in reduced and full dimensionality with ELVIBROT and TNUM
David Lauvergnat and André Nauts, Phys. Chem. Chem. Phys., 2010
DOI: 10.1039/c001944e

On the efficiency of treating singularities in triatomic variational vibrational computations. The vibrational states of H_3^+ up to dissociation†

Tamás Szidarovszky, Attila G. Császár and Gábor Czakó*‡

Received 19th January 2010, Accepted 14th April 2010
First published as an Advance Article on the web 4th June 2010
DOI: 10.1039/c001124j

Several techniques of varying efficiency are investigated, which treat all singularities present in the triatomic vibrational kinetic energy operator given in orthogonal internal coordinates of the two distances–one angle type. The strategies are based on the use of a direct-product basis built from one-dimensional discrete variable representation (DVR) bases corresponding to the two distances and orthogonal Legendre polynomials, or the corresponding Legendre-DVR basis, corresponding to the angle. The use of Legendre functions ensures the efficient treatment of the angular singularity. Matrix elements of the singular radial operators are calculated employing DVRs using the quadrature approximation as well as special DVRs satisfying the boundary conditions and thus allowing for the use of exact DVR expressions. Potential optimized (PO) radial DVRs, based on one-dimensional Hamiltonians with potentials obtained by fixing or relaxing the two non-active coordinates, are also studied. The numerical calculations employed Hermite-DVR, spherical-oscillator-DVR, and Bessel-DVR bases as the primitive radial functions. A new analytical formula is given for the determination of the matrix elements of the singular radial operator using the Bessel-DVR basis. The usually claimed failure of the quadrature approximation in certain singular integrals is revisited in one and three dimensions. It is shown that as long as no potential optimization is carried out the quadrature approximation works almost as well as the exact DVR expressions. If wave functions with finite amplitude at the boundary are to be computed, the basis sets need to meet the required boundary conditions. The present numerical results also confirm that PO-DVRs should be constructed employing relaxed potentials and PO-DVRs can be useful for optimizing quadrature points for calculations applying large coordinate intervals and describing large-amplitude motions. The utility and efficiency of the different algorithms is demonstrated by the computation of converged near-dissociation vibrational energy levels for the H_3^+ molecular ion.

I. Introduction

There are three principal approaches used for *exact* (within the given potential energy surface, PES) variational nuclear motion computations based on solving the time-independent (ro)vibrational Schrödinger equation. The first and most widely employed technique is based on internal coordinates and prederived, tailor-made Hamiltonians, see, *e.g.*, ref. 1, and usually requires the development of separate computer codes[2–8] for each new system. This approach has been mostly developed for triatomic and to some extent tetratomic systems and has been used to compute spectra of molecules exhibiting large-amplitude motions and even complete (up to the first dissociation limit) (ro)vibrational spectra.[9,10] The second, to some extent universal approach[11,12] does not require developing separate computer codes for molecules of different size and bonding arrangement and it is based on rectilinear normal coordinates and the Eckart–Watson Hamiltonian.[13] It can be used efficiently for semirigid molecules but quickly looses its effectiveness for treating large-amplitude motions and for systems with multiple minima. The third, fully numerical, universal, and almost 'black-box' approach[14–17] exhibits the favorable characteristics of the first two approaches, as it is built upon internal coordinates and is applicable to almost all full- or reduced-dimensional systems, coordinates, and coordinate embeddings using a single code. This approach is not yet ready for extremely demanding applications like the computation of the full spectrum, *i.e.*, the complete rotational–vibrational line-list of a molecule, which is one of the long-term goals of our research efforts. In what follows, the discussion concentrates on the first approach and only on triatomic systems, though generalizations of the results obtained will also be provided.

If so-called singular nuclear configurations, corresponding to singularities present in the kinetic energy operator, are

Laboratory of Molecular Spectroscopy, Institute of Chemistry, Eötvös University, P. O. Box 32, H-1518 Budapest 112, Hungary. E-mail: czako@chem.elte.hu

† Electronic supplementary information (ESI) available: Complete data tables showing vibrational energy levels of the H_3^+ molecular ion. See DOI: 10.1039/c001124j

‡ Current address: Cherry L. Emerson Center for Scientific Computation and Department of Chemistry, Emory University, Atlanta, GA 30322.

energetically accessible by the nuclear motions investigated, special care must be exercised to avoid the resulting numerical problems during variational computation of (ro)vibrational energy levels. Theoretical techniques that do not treat these singularities may result in unconverged eigenenergies; therefore, these methods cannot be employed when the goal is the determination of the complete (ro)vibrational spectrum.

There is a history of treatments offered to circumvent the radial singularity problem present in first-principles rovibrational spectroscopy. In 1993, Henderson, Tennyson, and Sutcliffe (HTS)[18] reanalyzed their 3-dimensional discrete variable representation (DVR) vibrational calculations in Jacobi coordinates for the H_3^+ molecular ion in order to find the source of the "nonvariational" behaviour of their results highlighted by Carter and Meyer.[19] The discrepancy was traced back to the failure of the standard quadrature approximation in certain integrals appearing during the DVR representation of the Hamiltonian. Different solution strategies of the radial singularity problem observed in Jacobi coordinates were proposed. The first, *a priori* solution strategy avoids the singularity problem by switching to a different coordinate system. One can use nonorthogonal valence coordinates (*i.e.*, two bond lengths and a bond angle). Valence coordinates, in comparison with Jacobi coordinates, are less well adapted to the potential, and despite their effective lack of singularities, they are a poor choice for very floppy molecules, like H_3^+.[6] Along the same line, Watson[20] advocated the use of hyperspherical coordinates[21] to avoid the radial singularity problem. Another, *a posteriori* strategy is based on the use of orthogonal coordinates, *e.g.* Jacobi coordinates, but with the proper treatment of the radial singularities. Two types of strategies should be mentioned. In the first approach, direct product of elementary basis functions having the proper boundary conditions are used and the matrix elements of the singular oparators are computed analytically, thus avoiding the use of the quadrature approximation. This strategy was followed by HTS utilizing the spherical oscillator functions and a successive contraction and diagonalization technique.[18] A similar strategy was followed by Bramley and Carrington[6] for the calculation of the vibrational energy levels of H_3^+ but using an iterative Lanczos approach. The second approach is based on appropriate nondirect-product bases designed to avoid the numerical consequences of the radial singularities. It is important to note that the radial singularity is coupled to the angular singularity, because when one of the radial coordinates becomes zero the Θ coordinate becomes undefined (see eqn (1) below). Therefore, an optimal basis is always a nondirect-product of functions depending on the coupled coordinates. Nevertheless, to the best of our knowledge there are only two techniques available that treat the singularities using a nondirect-product basis. Bramley *et al.*[22] advocated an approach that treats the radial singularity in a triatomic vibrational problem by using two-dimensional nondirect-product polynomial basis functions, which are the analytic eigenfunctions of the spherical harmonic oscillator Hamiltonian. In 2005 two of the authors of the present paper and their co-workers[23] advocated a similar nondirect-product basis method employing a generalized finite basis representation (GFBR) method[24] for the triatomic vibrational problem, whereby Bessel-DVR functions, developed by Littlejohn and Cargo,[25] were coupled to Legendre polynomials. This approach was further improved in 2006[26] and was augmented with the treatment of the rotational motion in 2007.[27]

Although an optimal basis for treating the singularity problem is a nondirect-product basis, the use of a direct-product basis, though it results in a longer expansion of the wave functions, has considerable advantages. First, the matrix elements of the potential energy operator can be computed more easily using a direct-product basis. Second, the structure of the Hamiltonian matrix is simpler if a direct-product basis is employed, allowing much more efficient coding of the matrix-vector multiplications required for an iterative eigensolver. (Note that this second problem hindered the use of the algorithms proposed in ref. 23, 26 and 27). In this paper different approaches based on direct-product basis sets will be considered, which would allow the efficient computation of the complete line-list of triatomic molecules. In 2006, using contracted basis functions and direct diagonalizations, computation of seemingly converged energies of all high-lying vibrational states of the H_3^+ molecular ion required the use of a large parallel supercomputer.[9,10] Therefore, it appears to be still necessary to further improve the efficiency of those techniques which can solve the time-independent (ro)vibrational Schrödinger equation while treating the important singularities and thus, in principle, are able to determine the full (ro)vibrational spectra of small molecules. This paper examines efficient *a posteriori* routes and makes recommendations on how to compute the full vibrational eigenspectrum of triatomic molecules at a modest cost. One should not forget that the ability to perform such calculations is also a requirement to compute the yet exotic resonance (quasibound) states of molecular systems *via* a bottom-up approach.

II. Theoretical background

Several strategies exist to set up a matrix representation of a vibrational Hamiltonian of triatomic molecules (see, *e.g.*, ref. 3–7, 18–20, 22 and 23). In the past two decades the use of orthogonal internal coordinate systems (O) became widespread because kinetic energy operators in orthogonal coordinates lack cross-derivative terms and thus have a very simple form. The Sutcliffe–Tennyson vibrational Hamiltonian of triatomic molecules[1] using orthogonal coordinates $\{R_1, R_2, \Theta\}$, *e.g.* Jacobi[28] or Radau[29] coordinates, is written in atomic units as

$$\hat{H} = -\frac{1}{2\mu_1}\frac{\partial^2}{\partial R_1^2} - \frac{1}{2\mu_2}\frac{\partial^2}{\partial R_2^2} - \left(\frac{1}{2\mu_1 R_1^2} + \frac{1}{2\mu_2 R_2^2}\right)\left(\frac{\partial^2}{\partial \Theta^2} + \cot\Theta\frac{\partial}{\partial \Theta}\right) + \hat{V}(R_1, R_2, \Theta), \quad (1)$$

where $\hat{V}$ is the potential energy operator, μ_1 and μ_2 are appropriately defined[1] mass-dependent constants, R_1 and R_2 denote the two stretching-type coordinates, Θ is a

bending-type coordinate, and the volume element for integration is $\sin\Theta dR_1 dR_2 d\Theta$.

The conceptually simplest variational techniques employ direct-product (P) basis sets for setting up the matrix representation of $\hat{H}$. Let us define a general three-dimensional, orthogonal and normalized direct-product basis as $\{\chi_{n_1}(R_1)\chi_{n_2}(R_2)\Phi_\ell(\cos\Theta)\}_{n_1=0,n_2=0,\ell=0}^{N_1-1,N_2-1,L-1}$, where the number of R_1-, R_2-, and Θ-dependent functions are N_1, N_2 and L, respectively. One can now build the $N_1N_2L\times N_1N_2L$-dimensional Hamiltonian as

$$\begin{aligned}\mathbf{H} = {} & \mathbf{K}_1^{N_1\times N_1}\otimes\mathbf{I}_2^{N_2\times N_2}\otimes\mathbf{I}_\Theta^{L\times L} + \mathbf{I}_1^{N_1\times N_1}\otimes\mathbf{K}_2^{N_2\times N_2}\otimes\mathbf{I}_\Theta^{L\times L} \\ & + \mathbf{R}_1^{N_1\times N_1}\otimes\mathbf{I}_2^{N_2\times N_2}\otimes\mathbf{K}_\Theta^{L\times L} \\ & + \mathbf{I}_1^{N_1\times N_1}\otimes\mathbf{R}_2^{N_2\times N_2}\otimes\mathbf{K}_\Theta^{L\times L} + \mathbf{V},\end{aligned} \tag{2}$$

where

$$(\mathbf{K}_j^{N_j\times N_j})_{n_j,n_j'} = \langle\chi_{n_j}(R_j)|-\frac{1}{2\mu_j}\frac{\partial^2}{\partial R_j^2}|\chi_{n_j'}(R_j)\rangle \qquad j=1 \text{ or } 2, \tag{3}$$

$$(\mathbf{R}_j^{N_j\times N_j})_{n_j,n_j'} = \langle\chi_{n_j}(R_j)|\frac{1}{2\mu_j R_j^2}|\chi_{n_j'}(R_j)\rangle \qquad j=1 \text{ or } 2, \tag{4}$$

$$(\mathbf{K}_\Theta^{L\times L})_{\ell,\ell'} = \langle\Phi_\ell(\cos\Theta)|-\left(\frac{\partial^2}{\partial\Theta^2}+\cot\Theta\frac{\partial}{\partial\Theta}\right)|\Phi_{\ell'}(\cos\Theta)\rangle, \tag{5}$$

the matrices $\mathbf{I}_1^{N_1\times N_1}$, $\mathbf{I}_2^{N_2\times N_2}$, and $\mathbf{I}_\Theta^{L\times L}$ mean $N_1\times N_1$-, $N_2\times N_2$-, and $L\times L$-dimensional unit matrices, respectively, and the elements of the $N_1N_2L\times N_1N_2L$-dimensional potential energy matrix are

$$(\mathbf{V})_{n_1n_2\ell,n_1'n_2'\ell'} = \langle\chi_{n_1}(R_1)\chi_{n_2}(R_2)\Phi_\ell(\cos\Theta)|V|\chi_{n_1'}(R_1)\chi_{n_2'}(R_2)\Phi_{\ell'}(\cos\Theta)\rangle. \tag{6}$$

Due to the appearance of the unit matrices in all the kinetic energy terms and assuming that $\mathbf{V}$ is not a full matrix, the matrix representation of the Hamiltonian results in an extremely sparse matrix of special structure whose eigenvalues can thus be obtained efficiently by an iterative (I) eigensolver. The above-described procedure, first advocated probably in ref. 6, is termed here OPI based on the abbreviations introduced. In almost all of the OPI techniques, building of the Hamiltonian matrix, whether done explicitly or not, cost negligible computer time and thus the time-determining step of these methods is the computation of the variational eigenpairs through a large number of matrix-vector multiplications. The speed of an iterative eigensolver depends on the sparsity and the structure of the Hamiltonian matrix. The number of nonzero elements of $\mathbf{H}$ depends on the choice of the basis functions and the employed integration techniques used for calculating elements of $\mathbf{R}_1^{N_1\times N_1}$, $\mathbf{R}_2^{N_2\times N_2}$, and $\mathbf{V}$ [see eqn (4) and (6)]. Therefore, in what follows different choices for the product basis functions will be considered.

II.1 D^{3}OPI

By employing DVR functions[30] for all three variables, one can set up the DVR representation of $\hat{H}$. The resulting procedure was termed DOPI in Ref. 4, where D stands for DVR and the other abbreviations have been defined above. For the purposes of the present discussion, let us call the DOPI technique D^{3}OPI, where the superscript 3 indicates that the DVR is employed in all three dimensions. Employing D^{3}OPI, the matrices $\mathbf{K}_1^{N_1\times N_1}$, $\mathbf{K}_2^{N_2\times N_2}$, and $\mathbf{K}_\Theta^{L\times L}$ have elements which can be obtained by analytical formulae,[30] while elements of the coordinate-dependent $\mathbf{R}_1^{N_1\times N_1}$ and $\mathbf{R}_2^{N_2\times N_2}$ matrices are calculated using the *quadrature approximation* resulting in a *diagonal* matrix representation. D^{3}OPI makes use of one of the principal advantages of the DVR representation, namely that the matrix $\mathbf{V}$ is diagonal. Nevertheless, since some of the off-diagonal matrix elements of $\mathbf{H}$ are non-zero anyway, this considerable simplification is not fully needed when the full representation of $\hat{H}$ is considered. The D^{3}OPI final Hamiltonian matrix is extremely sparse with only $(N_1+N_2+L-2)N_1N_2L$ nonzero elements, all at places known *a priori* (see the top panel of Fig. 1).

While the diagonal matrix representation of the $\hat{R}_1^{-2}$ and $\hat{R}_2^{-2}$ operators ensures that there are only a modest number of nonzero elements in $\mathbf{H}$, there might be a limitation for the application of D^{3}OPI due to the possible failure of the quadrature approximation when one of the radial coordinates goes to zero. It has generally been assumed[6,18] that one cannot use the quadrature approximation for calculating the integrals given in eqn (4) if one wants/needs to treat the radial singularities. Nevertheless, appropriate basis functions can be chosen which satisfy the boundary conditions, namely $\chi_{n_1}(R_1 = 0) = 0$ and $\chi_{n_2}(R_2 = 0) = 0$, allowing the exact computation of the matrix elements of the singular radial terms.

II.2 ED^{3}OPI

The D^{3}OPI protocol can be modified by choosing radial DVR bases in such a way that the integrals in eqn (4) are nonsingular and use analytical formulae for calculating the requested matrix elements. The resulting procedure is termed ED^{3}OPI, where E stands for the use of exact-DVR during the determination of the matrix representations of the singular operators. Due to the fact that the matrices $\mathbf{R}_1^{N_1\times N_1}$ and $\mathbf{R}_2^{N_2\times N_2}$ become full matrices, $\mathbf{H}$ will become a much less sparse matrix with $(N_1L+N_2L-L)N_1N_2L$ nonzero elements (see second panel of Fig. 1).

HTS[18] employed this technique and used spherical-oscillator DVR functions. However, they employed a successive diagonalization and truncation technique instead of an iterative eigensolver whereby the large increase in the number of nonzero Hamiltonian matrix elements requires different considerations. These computations proved to be considerably more expensive than those based on diagonal $\mathbf{R}_1^{N_1\times N_1}$ and $\mathbf{R}_2^{N_2\times N_2}$ matrices.

Thus, the question arises of how to treat the singularities without introducing extra matrix elements into the D^{3}OPI

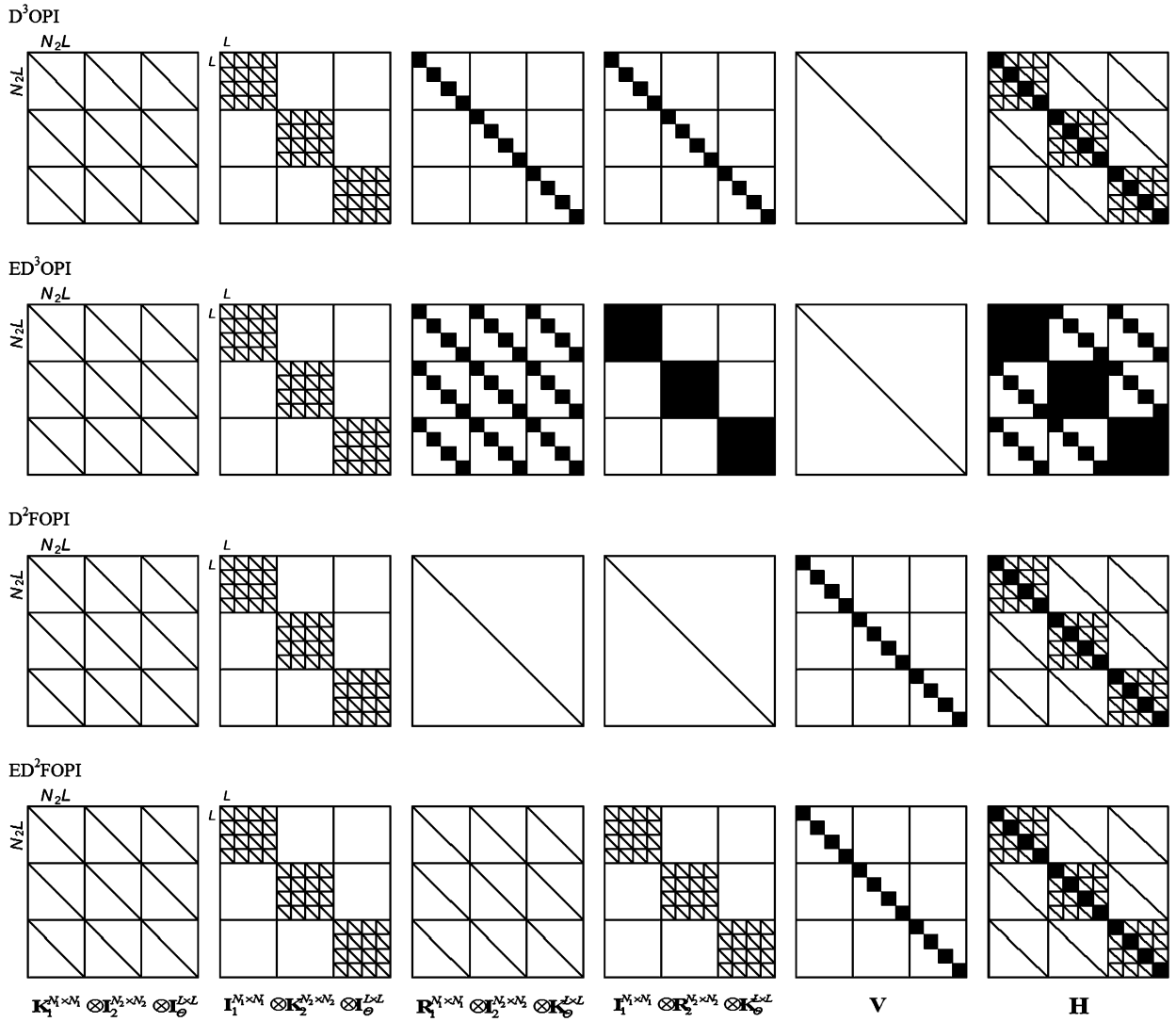

Fig. 1 Pictorial representation of the shape and the nonzero elements of the matrices appearing in eqn (2) corresponding to different procedures, namely, D^3OPI, ED^3OPI, D^2FOPI, and ED^2FOPI (for the sake of clarity, $N_1 = 3$ and $N_2 = 4$ have been chosen, see text).

Hamiltonian. For this, one has to look for a modification of the D^3OPI procedure which does not compromise the sparsity and structure of **H**.

II.3 D^2FOPI

One seemingly useful approach is to employ DVR only for the two radial coordinates and use a finite basis representation (FBR) for the coordinate Θ. This protocol can be termed D^2FOPI, where F stands for FBR in the angular dimension.

By employing the Legendre polynomials, $P_\ell(\cos\Theta)$, for describing the bending motion, advantage can be taken of the fact that the Legendre polynomials are the analytic eigenfunctions of the Θ-dependent part of the kinetic energy operator. Therefore, $\mathbf{K}_\Theta^{L\times L}$ is diagonal in this representation; thus, the matrices $\mathbf{R}_1^{N_1\times N_1}\otimes\mathbf{I}_2^{N_2\times N_2}\otimes\mathbf{K}_\Theta^{L\times L}$ and $\mathbf{I}_1^{N_1\times N_1}\otimes\mathbf{R}_2^{N_2\times N_2}\otimes\mathbf{K}_\Theta^{L\times L}$ are also diagonal. Naturally, when a mixed DVR-FBR technique is used, the potential energy matrix will cease to be diagonal. However, due to the 2D DVR, the matrix **V** remains block-diagonal, containing blocks of dimension $L\times L$ (third panel of Fig. 1). The matrix elements of **V** can be calculated using a Gauss–Legendre quadrature as

$$(\mathbf{V})_{n_1n_2\ell,n_1'n_2'\ell'} \cong \sum_{k=1}^{L} w_k P_\ell(q_k) V(r_{n_1}, r_{n_2}, q_k) P_{\ell'}(q_k)\delta_{n_1,n_1'}\delta_{n_2,n_2'}, \tag{7}$$

where w_k are the Gauss–Legendre quadrature weights corresponding to the quadrature points q_k. The points r_{n_1} and r_{n_2} correspond to the R_1- and R_2-dependent DVR bases, respectively. Most importantly, as can be seen in Fig. 1, no new nonzero matrix elements are introduced; the **H** matrix has exactly the same structure employing either D^3OPI or D^2FOPI.

II.4 ED^2FOPI

Finally, let us consider what happens if one does not use the quadrature approximation for calculating the elements of $\mathbf{R}_1^{N_1\times N_1}$ and $\mathbf{R}_2^{N_2\times N_2}$ within D^2FOPI. This method, where the integrals given in eqn (4) are obtained using exact-DVR

expressions and an FBR is used in 1D corresponding to the angular coordinate, is termed ED^{2}FOPI. Here, advantage can be taken of the properties of Legendre polynomials, which ensure that the matrices $\mathbf{K}_1^{N_1\times N_1}\otimes\mathbf{I}_2^{N_2\times N_2}\otimes\mathbf{I}_\Theta^{L\times L}$ and $\mathbf{I}_1^{N_1\times N_1}\otimes\mathbf{K}_2^{N_2\times N_2}\otimes\mathbf{I}_\Theta^{L\times L}$ have the same structure as the matrices $\mathbf{R}_1^{N_1\times N_1}\otimes\mathbf{I}_2^{N_2\times N_2}\otimes\mathbf{K}_\Theta^{L\times L}$ and $\mathbf{I}_1^{N_1\times N_1}\otimes\mathbf{R}_2^{N_2\times N_2}\otimes\mathbf{K}_\Theta^{L\times L}$, respectively. This means that no new nonzero matrix elements arise when all the singularities in eqn (1) are treated employing ED^{2}FOPI.

In summary, this exact-DVR technique, as well as D^{3}OPI and D^{2}FOPI result in exactly the same Hamiltonian matrix structure, with $(N_1+N_2+L-2)N_1N_2L$ nonzero elements (Fig. 1).

III. Efficiency of matrix-vector multiplications

The computational cost of an iterative eigensolver mostly depends on the speed of the multiplication of the matrix **H** with an arbitrary vector **v**. Consider an arbitrary full matrix of dimension $N_1N_2L\times N_1N_2L$. In this case the computational cost of a matrix-vector multiplication scales as $(N_1N_2L)^2$. Now, let us take advantage of the sparsity and special structure of **H** whereby the cost of a matrix-vector multiplication becomes proportional to the number of nonzero elements of **H** (see section II and Fig. 1).

In the case of a *direct-product* matrix an even more efficient matrix-vector multiplication can be employed, advocated in ref. 6, called sequential summation. An element of the product vector of the matrix **H** defined in eqn (2) and vector **v** is

$$\begin{aligned}(\mathbf{Hv})_{n_1n_2\ell}=\sum_{n_1'=0}^{N_1-1}\sum_{n_2'=0}^{N_2-1}\sum_{\ell'=0}^{L-1}[&(\mathbf{K}_1^{N_1\times N_1})_{n_1,n_1'}(\mathbf{I}_2^{N_2\times N_2})_{n_2,n_2'}(\mathbf{I}_\Theta^{L\times L})_{\ell,\ell'}\\&+(\mathbf{I}_1^{N_1\times N_1})_{n_1,n_1'}(\mathbf{K}_2^{N_2\times N_2})_{n_2,n_2'}(\mathbf{I}_\Theta^{L\times L})_{\ell,\ell'}\\&+(\mathbf{R}_1^{N_1\times N_1})_{n_1,n_1'}(\mathbf{I}_2^{N_2\times N_2})_{n_2,n_2'}(\mathbf{K}_\Theta^{L\times L})_{\ell,\ell'}\\&+(\mathbf{I}_1^{N_1\times N_1})_{n_1,n_1'}(\mathbf{R}_2^{N_2\times N_2})_{n_2,n_2'}(\mathbf{K}_\Theta^{L\times L})_{\ell,\ell'}\\&+(\mathbf{V})_{n_1n_2\ell,n_1'n_2'\ell'}](\mathbf{v})_{n_1'n_2'\ell'}.\end{aligned}\tag{8}$$

After some algebra, eqn (8) can be rearranged as

$$\begin{aligned}(\mathbf{Hv})_{n_1n_2\ell}=&\sum_{n_1'=0}^{N_1-1}(\mathbf{K}_1^{N_1\times N_1})_{n_1,n_1'}(\mathbf{v})_{n_1'n_2\ell}\\&+\sum_{n_2'=0}^{N_2-1}(\mathbf{K}_2^{N_2\times N_2})_{n_2,n_2'}(\mathbf{v})_{n_1n_2'\ell}\\&+\sum_{n_1'=0}^{N_1-1}(\mathbf{R}_1^{N_1\times N_1})_{n_1,n_1'}\sum_{\ell'=0}^{L-1}(\mathbf{K}_\Theta^{L\times L})_{\ell,\ell'}(\mathbf{v})_{n_1'n_2\ell'}\\&+\sum_{n_2'=0}^{N_2-1}(\mathbf{R}_2^{N_2\times N_2})_{n_2,n_2'}\sum_{\ell'=0}^{L-1}(\mathbf{K}_\Theta^{L\times L})_{\ell,\ell'}(\mathbf{v})_{n_1n_2'\ell'}\\&+\sum_{n_1'=0}^{N_1-1}\sum_{n_2'=0}^{N_2-1}\sum_{\ell=0}^{L-1}(\mathbf{V})_{n_1n_2\ell,n_1'n_2'\ell'}(\mathbf{v})_{n_1'n_2'\ell'}.\end{aligned}\tag{9}$$

Computing eqn (9) directly, in order to obtain **Hv**, one needs to perform $(N_1+N_2+N_1L+N_2L+N_1N_2L)N_1N_2L$ multiplications. However, if one introduces $\mathbf{v}'\in\Re^{N_1\times N_2\times L}$, where $(\mathbf{v}')_{n_1n_2\ell}=\sum_{\ell'=0}^{L-1}(\mathbf{K}_\Theta^{L\times L})_{\ell,\ell'}(\mathbf{v})_{n_1n_2\ell'}$, (computation of $\mathbf{v}'$ requires $N_1N_2L^2$ multiplications) and substitutes it in the third and fourth terms of eqn (9), one can compute **Hv** with $(N_1+N_2+N_1+N_2+N_1N_2L)N_1N_2L+N_1N_2L^2$ multiplications altogether. The relative decrease of the computational time can be significant if one uses a DVR-like method, where **V** is diagonal; thus, only $(N_1+N_2+N_1+N_2+1)N_1N_2L+N_1N_2L^2=(2N_1+2N_2+L+1)N_1N_2L$ multiplications are needed instead of $(N_1+N_2+N_1L+N_2L+1)N_1N_2L$.

When calculating **Hv** in the D^{3}OPI, D^{2}FOPI and ED^{2}FOPI representations, all the terms in eqn (9) have at most one sum, thus, the above introduced method cannot be used and the number of required multiplications scales with the number of nonzero elements $(N_1+N_2+L-2)N_1N_2L$. However, in the case of the ED^{3}OPI representation, where the third and fourth terms of eqn (9) have two sums, one can employ sequential summation, which decreases the computational cost significantly, since only $(2N_1+2N_2+L+1)N_1N_2L$ multiplications are required whereas the number of nonzero elements is $(N_1L+N_2L-L)N_1N_2L$.

IV. Radial basis functions

IV.1 Primitive basis functions

In section II the equations were given with arbitrary radial basis functions, *i.e.* $\chi_{n_j}(R_j)$, and the actual forms of these functions were not specified. During the present study three radial basis sets were considered.

The first is the Hermite-DVR basis,[30] with corresponding spectral basis functions

$$\chi_{n_j}^{\mathrm{VBR}}(R_j)=N_{n_j}H_{n_j}(K_j(R_j-R_{j,0}))e^{-K_j^2(R_j-R_{j,0})^2/2},\tag{10}$$

where

$$N_{n_j}=\sqrt{\frac{K_j}{2^{n_j}n_j!\sqrt{\pi}}},$$

H_{n_j} is the n_jth Hermite polynomial, $K_j=2q_{N_j}^{K_j=1}/(R_j^{\max}-R_j^{\min})$ and $R_{j,0}=(R_j^{\min}+R_j^{\max})/2$, where $q_{N_j}^{K_j=1}$ is the largest eigenvalue of $\mathbf{Q}_j$ (see below) with $K_j=1$ (largest appropriate Gaussian quadrature point), and $R_j^{\min}$ and $R_j^{\max}$ are free parameters. The Hermite-DVR basis can be set up *via* the so-called transformation method.[31] The coordinate matrices are defined as

$$(\mathbf{Q}_j)_{n_j,n_j'}=\langle\chi_{n_j}^{\mathrm{VBR}}(R_j)|R_j|\chi_{n_j'}^{\mathrm{VBR}}(R_j)\rangle,\ j=1\text{ or }2.\tag{11}$$

The eigenvalues of $\mathbf{Q}_j$ provide the radial quadrature points, while the eigenvectors, ordered in a matrix, $\mathbf{T}_j$, form the transformation matrix, which is used to set up the DVR of the differential operators. The definition of K_j ensures that all the quadrature points are in the interval $[R_j^{\min},\ R_j^{\max}]$. This basis does not satisfy the $\chi_{n_j}(R_j=0)=0$ boundary conditions; thus, the integral defined in eqn (4) becomes singular and cannot be computed analytically.

The second basis set is based on the spherical-oscillator functions

$$\chi_{n_j}^{\mathrm{VBR}}(R_j) = N_{n_j,\alpha+1/2} 2^{1/2} K_j^{1/4} (K_j R_j^2)^{(\alpha+1)/2} \times e^{-K_j R_j^2/2} L_{n_j}^{\alpha+1/2}(K_j R_j^2), \quad (12)$$

where α is a free parameter, $L_{n_j}^{\alpha+1/2}$ is an associated Laguerre polynomial, $N_{n_j,\alpha+1/2}$ is the norm of $L_{n_j}^{\alpha+1/2}$, $K_j = q_{N_j}^{(2),K_j=1}/(R_j^{\max})^2$, where $q_{N_j}^{(2),K_j=1}$ is the largest eigenvalue of $\mathbf{Q}_j^{(2)}$ (see below) if $K_j = 1$ (largest appropriate Gaussian quadrature point), and $R_j^{\max}$ is a free parameter. The DVR is set up similarly to the Hermite-DVR; however, the matrix of the square of the coordinate is employed,

$$(\mathbf{Q}_j^{(2)})_{n_j,n_j'} = \langle \chi_{n_j}^{\mathrm{VBR}}(R_j) | R_j^2 | \chi_{n_j'}^{\mathrm{VBR}}(R_j) \rangle, \; j = 1 \text{ or } 2. \quad (13)$$

thus, the quadrature points are the square roots of the eigenvalues of $\mathbf{Q}_j^{(2)}$. The definition of K_j ensures that all the quadrature points are in the interval (0, $R_j^{\max}$]. This basis for $\alpha = 0$ satisfies the boundary conditions of the problem, *i.e.*, $\chi_{n_j}(R_j = 0) = 0$, and results in non-singular integrals in eqn (4) for all $\alpha \geq 0$; thus, eqn (4) can be obtained *via* an exact DVR expression as in ref. 18. In this case, the exact FBR, *i.e.* the variational basis representation (VBR) of eqn (3) and (4) can be obtained analytically as[18,32]

$$(\mathbf{K}_j^{\mathrm{VBR}})_{n_j,n_j'} = -\frac{1}{2\mu_j}\frac{K_j}{2} N_{n_j,\alpha+1/2} N_{n_j',\alpha+1/2} \times \left[(2n_j+\alpha+3/2)\frac{\Gamma(n_j+\alpha+3/2)}{n_j!}\delta_{n_j,n_j'} + \frac{\Gamma(n_j+\alpha+3/2)}{n_j'!}\delta_{n_j-1,n_j'} + \frac{\Gamma(n_j'+\alpha+3/2)}{n_j!}\delta_{n_j,n_j'-1} - \alpha(\alpha+1)\sum_{\lambda=0}^{\min(n_j,n_j')}\frac{\Gamma(\lambda+\alpha+1/2)}{\lambda!}\right] \quad (14)$$

$$(\mathbf{R}_j^{\mathrm{VBR}})_{n_j,n_j'} = \frac{K_j}{2\mu_j}\sqrt{\frac{n_j!\Gamma(n_j'+\alpha+3/2)}{n_j'!\Gamma(n_j+\alpha+3/2)}}, \; n_j \geq n_j', \quad (15)$$

respectively, and the analytic elements of the coordinate matrix defined in eqn (13) are

$$(\mathbf{Q}_j^{(2)})_{n_j,n_j'} = N_{n_j,\alpha+1/2} N_{n_j',\alpha+1/2} K_j^{-1} \times \left[\left(\frac{\Gamma(n_j+\alpha+5/2)}{n_j!} + \frac{\Gamma(n_j+\alpha+3/2)}{(n_j-1)!} \right)\delta_{n_j,n_j'} - \frac{\Gamma(n_j+\alpha+5/2)}{n_j!}\delta_{n_j,n_j'-1} - \frac{\Gamma(n_j+\alpha+3/2)}{(n_j-1)!}\delta_{n_j-1,n_j'} \right]. \quad (16)$$

The exact DVRs of eqn (3) and (4) are $\mathbf{K}_j^{N_j\times N_j} = (\mathbf{T}_j^{(2)})^{\mathrm{T}}\mathbf{K}_j^{\mathrm{VBR}}\mathbf{T}_j^{(2)}$ and $\mathbf{R}_j^{N_j\times N_j} = (\mathbf{T}_j^{(2)})^{\mathrm{T}}\mathbf{R}_j^{\mathrm{VBR}}\mathbf{T}_j^{(2)}$, respectively, where the transformation matrix, $\mathbf{T}_j^{(2)}$, contains the eigenvectors of $\mathbf{Q}_j^{(2)}$.

The third basis set employs the Bessel-DVR functions[25] defined as

$$\chi_{n_j}(R_j) = (-1)^{n_j+1}\frac{K_j(n_j+1)\pi\sqrt{2R_j}}{(K_jR_j)^2-(n_j+1)^2\pi^2} J_{1/2}(K_jR_j), \quad (17)$$

where $J_{1/2}(K_jR_j)$ is a Bessel function of the first kind and $K_j = N_j\pi/R_j^{\max}$. The set of Bessel grid points is defined as $r_{n_j} = (n_j + 1)\pi/K_j$, thus all the grid points are in the interval $0 < r_{n_j} \leq R_j^{\max}$, where $R_j^{\max}$ is a free parameter used to define the ranges of the R_j coordinates. To the best of the authors' knowledge these Bessel-DVR functions have not been used as a direct product basis in triatomic vibrational calculations.

When employing the Bessel-DVR basis the analytic matrix elements of the matrices defined in eqn (3) and (4) are obtained as follows:

$$(\mathbf{K}_j^{N_j\times N_j})_{n_j,n_j'} = \delta_{n_j,n_j'}\frac{1}{2\mu_j}\frac{K_j^2}{3}\left(1-\frac{3}{2(n_j+1)^2\pi^2}\right) + (1-\delta_{n_j,n_j'})\frac{(-1)^{n_j-n_j'}}{2\mu_j}\frac{8K_j^2}{\pi^2}\frac{(n_j+1)(n_j'+1)}{[(n_j+1)^2-(n_j'+1)^2]^2} \quad (18)$$

and

$$(\mathbf{R}_j^{N_j\times N_j})_{n_j,n_j'} = \frac{(-1)^{n_j+n_j'}}{2\mu_j}\frac{K_j^2}{\pi^2}\left(\frac{1}{(n_j+1)^2}\delta_{n_j,n_j'} + \frac{2}{(n_j+1)(n_j'+1)}\right). \quad (19)$$

It is important to note that using the standard quadrature approximation one would write $(\mathbf{R}_j^{N_j\times N_j})_{n_j,n_j'} \cong 1/(2\mu_j)K_j^2/[(n_j+1)^2\pi^2]\delta_{n_j,n_j'}$, whereas a newly derived exact formula given in eqn (19) results in a non-diagonal matrix representation. In other words, similarly to the spherical-oscillator-DVR, the Bessel-DVR functions satisfy the required boundary conditions allowing the analytic calculation of the matrix elements of the singular radial operators.

IV.2 Potential optimized DVR

In order to make the matrix representation of $\hat{H}$ as compact as possible *without modifying the structure* of **H**, the so-called potential optimized (PO) DVR[33–35] method can be employed. The PO-DVR approach employed in this study for the stretching coordinates can be described briefly as follows.

First, solve the eigenvalue problems of the following one-dimensional Hamiltonians using a large number of points:

$$\hat{H}_j^{1\mathrm{D}} = -\frac{1}{2\mu_j}\frac{d^2}{dR_j^2} + \frac{\ell(\ell+1)}{2\mu_jR_j^2} + \hat{V}(R_j; R_{j'}, \Theta) \quad j,j' = 1,2 \text{ or } 2,1 \quad (20)$$

where $\ell = 0$ for even-parity and $\ell = 1$ for odd-parity calculations. In this study two different one-dimensional effective potential function, $\hat{V}(R_j; R_{j'}, \Theta)$, were considered. In the first approach, coordinates $R_{j'}$ and Θ are fixed parameters, usually taken as the equilibrium values. In the second approach, a relaxed potential is employed, *i.e.* $\hat{V}(R_j; R_{j'}, \Theta)$ is obtained by optimizing the $R_{j'}$ and Θ coordinates for each value of R_j.

The PO spectral basis functions are the first couple of eigenfunctions of $\hat{H}_j^{1D}$. The choice of $\ell = 0$ for even-parity and $\ell = 1$ for odd-parity states in the one-dimensional Hamiltonian is made to adjust the boundary behavior of the PO spectral basis functions to the boundary properties of the three-dimensional wave functions (for details on boundary properties see section V and VI.1). Test calculations on the vibrational energy levels of H_3^+ show that using $\ell = 1$ for even-parity and $\ell = 0$ for odd-parity states results in an increase of the average error of the band origins above the barrier to linearity by a few tens of cm^{-1} for even-parity and a few cm^{-1} for odd-parity states.

Next, set up the PO-DVR representation *via* the transformation method along the following steps.

(*i*) Since the spherical-oscillator-DVR and the Bessel-DVR functions diagonalize the matrix of the square of the coordinate operator, the matrix representation of R_j^2, $\mathscr{Q}_j^{(2)}$, is set up using the first couple of eigenfunctions of $\hat{H}_j^{1D}$. The PO quadrature points are the square roots of the eigenvalues of $\mathscr{Q}_j^{(2)}$. The transformation matrix, $\mathscr{T}_j^{(2)}$, contains the eigenvectors of $\mathscr{Q}_j^{(2)}$. In the case of the Hermite-DVR the matrix representation of R_j, $\mathscr{Q}_j$, is set up using the first couple of eigenfunctions of $\hat{H}_j^{1D}$ and the eigenvalues and eigenvectors of $\mathscr{Q}_j$ are the PO quadrature points and the transformation matrix $\mathscr{T}_j$, respectively.

(*ii*) Since the eigenfunctions of $\hat{H}_j^{1D}$ are linear combinations of the $\chi_{n_j}(R_j)$ primitive DVR functions, the "PO-VBR" representation of the kinetic energy operator can be simply obtained analytically.

(*iii*) The kinetic energy matrix is transformed from "PO-VBR" to PO-DVR by a unitary transformation employing the matrix $\mathscr{T}_j$ or $\mathscr{T}_j^{(2)}$.

(*iv*) The matrix elements of the potential are calculated using the new PO-DVR grid points as radial quadrature points.

V. One-dimensional tests

In order to gain a better understanding of the consequences of the choice of basis sets satisfying or neglecting the boundary conditions characterizing the system under investigation and the quadrature or exact DVR approximations, it is worth first considering some model one-dimensional tests.

Consider the following one-dimensional Schrödinger equation,

$$\left(-\frac{1}{2}\frac{d^2}{dR^2}-\frac{1}{R}\frac{d}{dR}+\frac{\ell(\ell+1)}{2R^2}+\frac{1}{2}R^2\right)\psi_n(R)=E_n\psi_n(R), \tag{21}$$

where $R \in [0, \infty)$ and the integration volume element is R^2dR. Eqn (21) can be solved analytically for each $\ell = 0, 1, 2, \ldots$, and the eigenvalues are $E_n = 2n + \ell + 3/2$. The eigenfunctions, $\psi_n(R)$, have zero amplitude at $R = 0$, with the sole exception of the $\ell = 0$ case (in which case there is no R^{-2} singular term). It is straightforward to show that solution of the following ordinary differential equation,

$$\left(-\frac{1}{2}\frac{d^2}{dR^2}+\frac{\ell(\ell+1)}{2R^2}+\frac{1}{2}R^2\right)\phi_n(R)=E_n\phi_n(R), \tag{22}$$

with the integration volume element of dR gives the same eigenvalues as eqn (21). It is important to note that the eigenfunctions of eqn (22) are the eigenfunctions of eqn (21) multiplied by R, that is $\phi_n(R)/R = \psi_n(R)$. Thus the matrix representation of the Hamiltonian in eqn (22) with a given basis set is equivalent with the matrix representation of the Hamiltonian in eqn (21) with the same basis functions divided by the R coordinate.

In this work, the matrix representations of eqn (22) were obtained using the three different radial basis sets defined in section IV.1 using either the quadrature approximation or the exact-DVR representation, if possible, for the term involving R^{-2}.

Although the Hermite-DVR basis functions are orthogonal and normalized in the coordinate space $R \in (-\infty, \infty)$, with proper R_0 and K choices these functions are numerically zero at $R \leq 0$, thus are appropriate for the present model problem with $R \in [0, \infty)$.

Dividing the basis functions defined in section IV.1 by the R coordinate, one obtains the "equivalent" basis functions for eqn (21), as discussed above. When divided by the R coordinate, the spherical oscillator functions with $\alpha = 0$ and the Bessel-DVR functions have finite values at $R = 0$, the spherical oscillator functions with $\alpha = 1$ are zero at $R = 0$, while the Hermite-DVR functions diverge at $R = 0$, thus the latter two have improper boundary conditions (if $\ell = 0$ and $\alpha = 1$). Naturally, the approximate eigenfunctions of eqn (21) built from these basis sets will have the same boundary properties.

As seen in Table 1, when using basis functions with proper boundary conditions the eigenvalues converge in all $\ell = 0, 1, 2, \ldots$ cases with both the exact-DVR and the quadrature approximation for the term involving R^{-2}. Using the quadrature approximation, convergence is slightly slower. The results obtained with basis functions having improper boundary conditions are in good agreement with what one would expect from their boundary properties. Applying the spherical oscillator functions with $\alpha = 1$, eigenvalues seem to converge in all $\ell = 0, 1, 2, \ldots$ cases, but extremely slowly for $\ell = 0$ since at $R = 0$ the basis functions vanish, although the wavefunction has a finite amplitude. Using the Hermite-DVR, only $\ell \geq 1$ cases converge, the DVR matrix elements of the singular term can only be evaluated *via* the quadrature approximation, since the matrix elements in the FBR representation diverge.

These results show that (a) the matrix representation of the singular term can be given using either the approximate or the exact DVR representation, and (b) if the wave function has a finite amplitude at the boundary ($\ell = 0$ case), naturally, use of basis sets with improper boundary conditions leads to unconverged (or extremely slowly converging) eigenvalues. The applicability of the quadrature approximation confronts the usual claim that the quadrature approximation fails when used in the case of the singular term involving R^{-2}. It is of general interest to state that even if basis functions with improper boundary conditions are used, with which the wave function cannot possibly be correctly approximated, converged eigenvalues can be obtained if the wave function has zero amplitude at the boundary ($\ell \geq 1$ case). This reflects the fact that the basis functions only need to describe the wave

Table 1 Eigenvalues corresponding to the solution of the one-dimensional Schrödinger equation [eqn (22)] obtained with three different radial DVR basis sets (Hermite-DVR, spherical-oscillator-DVR ($\alpha = 0, 1$), and Bessel-DVR) using either the quadrature approximation (Appr.) or the exact-DVR (E-DVR) for the singular R^{-2} term[a]

	$N = 15$[b]							$N = 40$[b]							
	Hermite	Spherical $\alpha = 0$		Spherical $\alpha = 1$		Bessel		Hermite	Spherical $\alpha = 0$		Spherical $\alpha = 1$		Bessel		
	Appr.	Appr.	E-DVR	Appr.	E-DVR	Appr.	E-DVR	Appr.	Appr.	E-DVR	Appr.	E-DVR	Appr.	E-DVR	Exact
$\ell = 0$															
0	*0.647*	1.500		*1.638*		1.500		*1.013*	1.500		*1.547*		1.500		1.5
1	*2.132*	3.500		*3.711*		3.500		*2.741*	3.500		*3.571*		3.500		3.5
2	*3.940*	5.500		*5.774*		5.501		*4.553*	5.500		*5.589*		5.500		5.5
3	*6.018*	7.500		*7.836*		7.515		*6.413*	7.500		*7.604*		7.500		7.5
4	*8.343*	9.501		*9.911*		9.628		*8.305*	9.500		*9.617*		9.500		9.5
5	*10.910*	11.512		*12.025*		12.021		*10.222*	11.500		*11.629*		11.500		11.5
$\ell = 1$															
0	2.428	2.480	2.511	2.450	2.500	2.464	2.520	2.496	2.499	2.500	2.498	2.500	2.499	2.501	2.5
1	4.295	4.439	4.530	4.370	4.500	4.382	4.565	4.489	4.498	4.501	4.494	4.500	4.496	4.502	4.5
2	6.256	6.368	6.562	6.280	6.500	6.222	6.665	6.479	6.496	6.502	6.489	6.500	6.493	6.503	6.5
3	8.482	8.253	8.616	8.199	8.500	7.977	8.886	8.466	8.494	8.503	8.483	8.500	8.489	8.505	8.5
4	10.995	10.081	10.721	10.153	10.500	9.842	11.295	10.450	10.492	10.504	10.476	10.500	10.485	10.507	10.5
5	13.780	11.873	12.939	12.178	12.512	12.118	13.811	12.432	12.489	12.505	12.469	12.500	12.479	12.510	12.5

[a] All calculations were performed with $R^{max} = 10.00$ bohr, while $R^{min} = 0.05$ bohr was set for the Hermite-DVR. It is noted that although the spherical-oscillator functions with $\alpha = \ell$ are the analytic solutions of eqn (22), discrepancies compared to the exact results occur due to the fixing of the parameter R^{max}. Numbers suffering from convergence problems are indicated in italics. [b] N stands for the number of basis functions, *i.e.* grid points.

function in the regions of physical interest and not in the whole coordinate space.

VI. A three-dimensional test: all the bound vibrational levels of H_3^+

In 2006, Tennyson and co-workers[9,10] computed almost all of the vibrational energy levels corresponding to the electronic ground state of the H_3^+ molecular ion. This was the first study for H_3^+ whereby the PES employed had the correct dissociative behavior. A short summary of the relevant results of ref. 9 and 10 are as follows. (1) The first dissociation energy (D_0) of H_3^+, which corresponds to the breakup $H_3^+ \rightarrow H_2 + H^+$, is 34 911.6 cm^{-1}. (2) Below D_0, this PES supports 687 even-parity and 599 odd-parity vibrational states. (3) All but one state below D_0 were claimed to be converged to better

Table 2 Average absolute discrepancies in the given energy intervals between the reference (ref. 10) and the incomplete basis set vibrational energy levels of H_3^+, all in cm^{-1}, computed with different *primitive* basis sets using either the quadrature approximation (Appr.) or the exact-DVR (Exact) for the singular term in the Jacobi coordinate system[a]

	$(N_1\ N_2\ L) = (85\ 80\ 30)$													
	Hermite		Spherical (0,0)[b]				Spherical (0,1)[b]				Bessel			
	Appr.		Appr.		Exact		Appr.		Exact		Appr.		Exact	
Interval	Even	Odd	Even	Odd	Even	Odd	Even	Odd	Even	Odd	Even	Odd	Even	Odd
0–10 000	*0.21*	*0.15*	0.00	0.00	0.00	0.00	0.00	0.00	0.00	0.00	0.00	0.00	0.00	0.00
10 000–20 000	*92.53*	*1.02*	0.03	0.16	0.02	0.05	*6.75*	0.42	*6.76*	0.02	0.02	0.26	0.01	0.13
20 000–25 000	*143.18*	*11.89*	0.12	0.57	0.12	0.14	*11.48*	1.49	*11.51*	0.11	0.08	0.90	0.07	0.47
25 000–30 000	*143.19*	*21.68*	0.32	1.00	0.32	0.18	*11.06*	2.34	*11.12*	0.30	0.59	1.66	0.34	0.63
30 000–34 912	*124.60*	*17.92*	1.09	1.63	1.09	0.43	*10.59*	3.24	*10.70*	0.75	1.37	2.82	1.08	0.80
	$(N_1\ N_2\ L) = (95\ 90\ 35)$													
	Hermite		Spherical (0,0)[b]				Spherical (0,1)[b]				Bessel			
	Appr.		Appr.		Exact		Appr.		Exact		Appr.		Exact	
	Even	Odd	Even	Odd	Even	Odd	Even	Odd	Even	Odd	Even	Odd	Even	Odd
0–10 000	*0.01*	*0.02*	0.00	0.00	0.00	0.00	0.00	0.00	0.00	0.00	0.00	0.00	0.00	0.00
10 000–20 000	*63.82*	*0.81*	0.02	0.11	0.02	0.03	*5.98*	0.30	*5.99*	0.02	0.01	0.17	0.01	0.10
20 000–25 000	*114.62*	*3.73*	0.10	0.40	0.10	0.09	*10.16*	1.05	*10.18*	0.09	0.05	0.60	0.05	0.34
25 000–30 000	*120.72*	*4.45*	0.28	0.74	0.28	0.14	*9.78*	1.68	*9.81*	0.27	0.14	1.00	0.14	0.41
30 000–34 912	*122.66*	*9.93*	1.04	1.28	1.04	0.44	*9.39*	2.42	*9.45*	0.70	0.82	1.57	0.81	0.43

[a] All calculations were performed with $R_1^{max} = 14.00$ bohr, $R_2^{max} = 8.00$ bohr, and $m(H) = 1.007825\ u$. For Hermite-DVR $R_j^{min} = 0.05$ bohr ($j = 1, 2$) was used. ($N_1\ N_2\ L$) stands for using N_1, N_2, and L basis functions for the R_1, R_2, and Θ coordinates, respectively. Numbers suffering from convergence problems are indicated in italics. [b] "Spherical (n,m)" stands for spherical-oscillator-DVR radial basis sets with $\alpha = n$ and m for the R_1 and R_2 Jacobi coordinates, respectively.

than 1 cm^{-1}. (4) In order to obtain these (nearly) converged results for the high-lying vibrational states of H_3^+, at the time of the study the use of a large parallel supercomputer with a couple of hundred processors was required.

The ground-state PES used in our study and taken from ref. 10 is called PPKT2, which is an adjusted version of the former PPKT PES of ref. 36. The same masses as in ref. 10 were employed, making comparison of our results with those of Munro and co-workers[10] straightforward. Note also that Munro *et al.*[10] employed Radau coordinates, whereas all the computations of the present study have been performed in the Jacobi coordinate system, where the $R_2 = 0$ singularity comes into play much sooner, at the barrier to linearity, which is only about 9 950 cm^{-1} above the ZPVE of H_3^+. In what follows, we use the vibrational levels of ref. 10 as reference values.

VI.1 Test of the quadrature approximation

In the first set of test computations, the vibrational energy levels of H_3^+ up to the first dissociation limit have been computed using the *primitive* basis sets defined in section IV.1. The computations applied either exact-DVR (the ED^2FOPI representation) or the quadrature approximation (the D^2FOPI representation) during the evaluation of the singular matrix elements defined in eqn (4). The results obtained are summarized in Table 2. Wave functions corresponding to even-parity energy levels larger than the barrier to linearity might have finite amplitude at $R_2 = 0$. In correspondence with 1D results, eigenvalues obtained with basis sets having *improper boundary conditions* for the even-parity states, *i.e.* Hermite-DVR and spherical oscillator-DVR with $\alpha = 1$, show huge average errors in the even-parity levels for energy regions above the barrier to linearity. Also in agreement with the 1D experience, computations using the quadrature approximation seem to give the same results as the ones using exact-DVR, but with slightly slower convergence rate, especially for the odd-parity states. Here it is noted that near the dissociation energy (D_0), a few lines are missing completely for all the *primitive* basis sets. This is due to setting the $R_j^{max}, j \in \{1, 2\}$ parameters too small, *i.e.* $R_1^{max} = 14.00$ and $R_2^{max} = 8.00$ bohr; thus, the quadrature points are not sampled from areas where diffuse wave functions might still have substantial amplitudes. A study of such diffuse states is given in ref. 10 and 37. As seen in Table S1 of the ESI,† increasing the R_j^{max} parameters to larger values, *i.e.* $R_1^{max} = R_2^{max} = 17.65$ bohr, leads to noticeable errors, the number of quadrature points (DVR basis functions) for such large coordinate ranges is insufficient to achieve converged results using primitive DVR basis sets. (The proper PO-DVR computations give the complete set of states as discussed in section VI.2).

As expected, the Hermite-DVR gives much worse even-parity results than odd levels; however, the odd energies

Table 3 Average absolute discrepancies in the given energy intervals between the reference (ref. 10) and the incomplete basis set vibrational energy levels of H_3^+, all in cm^{-1}, computed with *primitive* and *PO* Bessel-DVR bases using exact-DVR and either the "fixed" or "relaxed" potentials in the one-dimensional Hamiltonians in the Jacobi coordinate system[a]

	$(N_1\ N_2\ L) = (85\ 80\ 30)$					
	Primitive		PO (fix)		PO (relax)	
Interval	Even	Odd	Even	Odd	Even	Odd
0–10 000	0.00	0.00	0.44	0.00	0.00	0.00
10 000–20 000	0.01	0.13	152.73	43.01	0.03	0.03
20 000–25 000	0.07	0.47	302.35	156.27	0.15	0.13
25 000–30 000	0.34	0.63	354.29	213.19	0.45	0.38
30 000–34 912	1.08	0.80	363.72	242.92	1.19	1.06
	$(N_1\ N_2\ L) = (95\ 90\ 35)$					
	Primitive		PO (fix)		PO (relax)	
	Even	Odd	Even	Odd	Even	Odd
0–10 000	0.00	0.00	0.24	0.00	0.00	0.00
10 000–20 000	0.01	0.10	133.32	36.94	0.01	0.02
20 000–25 000	0.05	0.34	260.28	131.64	0.05	0.06
25 000–30 000	0.14	0.41	302.24	176.45	0.16	0.12
30 000–34 912	0.81	0.43	310.72	201.60	0.47	0.43

[a] All calculations were performed with $m(H) = 1.007825\ u$. For calculations with PO basis $R_j^{max} = 17.65$ bohr ($j = 1, 2$), for calculations with primitive basis $R_1^{max} = 14.00$ and $R_2^{max} = 8.00$ bohr were used. During the PO-DVR 500 primitive basis functions were included for both stretching-type coordinates. Constrained coordinate values for the fixed-PO-DVRs were as follows: $R_1 = 1.649990$, $R_2 = 1.428930$ bohr, and $\cos(\Theta) = 0$. $(N_1\ N_2\ L)$ stands for using N_1, N_2, and L basis functions for the R_1, R_2, and Θ coordinates, respectively.

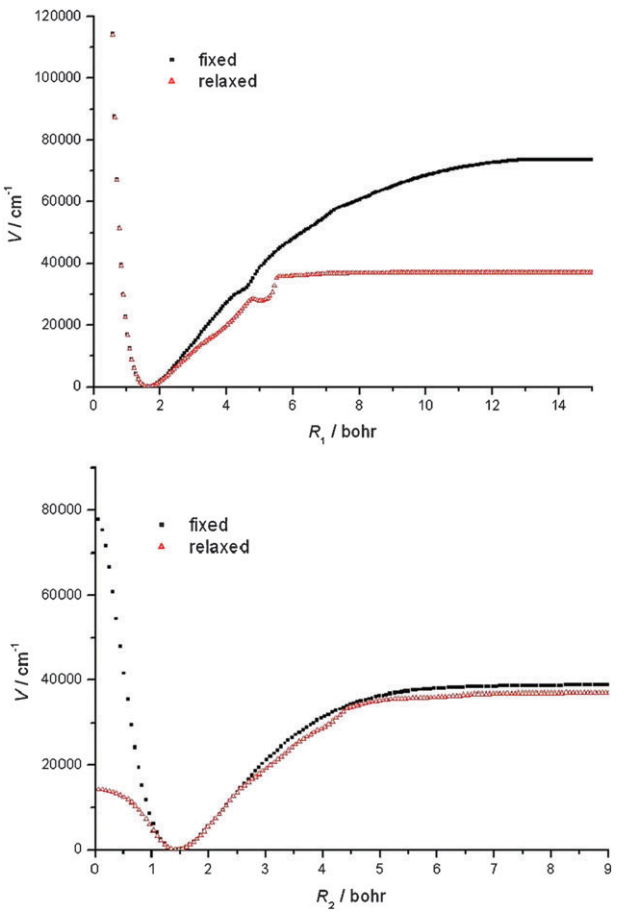

Fig. 2 Pictorial representation of the effective one-dimensional potentials of H_3^+ in Jacobi coordinates obtained by fixing at equilibrium (squares) or relaxing (triangles) the other two non-active coordinates [see eqn (20)].

are unconverged as well. The poor results obtained with Hermite-DVR for odd-parity states (including band origins under the barrier to linearity as well) can be greatly improved by optimizing (increasing) the $R_j^{\min}$ parameters; however, for even-parity states this does not reduce the error introduced by the improper boundary properties.

On the basis of the results obtained with *primitive* DVRs, the following can be stated. If one were to compute (ro)vibrational energy levels with wave functions having a finite amplitude at the boundary, basis sets with *proper* boundary conditions need to be used. Then, both the quadrature approximation and the exact-DVR can be applied for the evaluation of the singular terms, even when the wave function does not vanish at the singular nuclear configurations. The use of exact-DVR is recommended because of faster convergence, unless the quadrature approximation results in major computational benefits.

VI.2 Test of the PO-DVR

Computations for testing the properties and usefulness of potential optimized basis functions, introduced in section IV.2, have also been carried out. Table 3 shows the comparison of results obtained by primitive Bessel-DVR and PO Bessel-DVR both with "fixed" (at equilibrium) and "relaxed" potentials [see eqn (20)]. The different one-dimensional effective potentials for H_3^+ are shown in Fig. 2. Table 4 summarizes the results computed using PO basis sets, obtained from "relaxed" effective potentials, built from the different radial functions introduced in section IV.1, and calculated *via* both the quadrature approximation and the exact-DVR (if the latter exists).

PO-DVR can supply more compact basis functions compared to the primitive basis set; thus, faster convergence can be expected. However, it is clear from Table 3 that great caution is warranted when using PO-DVR. Although much faster convergence has been experienced for low-energy eigenstates with both "fixed" and "relaxed" PO-DVRs, eigenvalues with energies above 10 000 cm^{-1} relative to the ZPVE have huge errors if the "fixed" PO-DVR is used. Concerning the full spectra, "relaxed" PO-DVR computations show faster convergence than the corresponding primitive basis sets, as long as exact-DVR is used. The advantage of the "relaxed" PO-DVR is especially pronounced when the $R_j^{\max}$ parameters are set large enough for calculating the highly diffuse states, as these were missing from the *primitive* basis set calculations at lower $R_j^{\max}$ values. It is important to emphasize that the use of the PO-DVR, based on effective potentials obtained by fixing the non-active coordinates at their equilibrium values, can be advantageous for the low-lying levels (the "relaxed" PO-DVR is even better);[14] however, this method should not be employed if the computation of the *complete* spectrum is the goal. Fig. 2 clearly shows that the R_1-dependent effective potential gives improper dissociation behavior and the R_2-dependent potential hinders the sampling of the PO quadrature points in the near-zero region if the frozen coordinates are at equilibrium. The latter problem was realized by Bramley and Carrington,[6] who suggested fixing the R_1 Jacobi coordinate at 1.5 Å (the equilibrium value is about 0.87 Å); thus, the R_2-dependent effective potential had a

Table 4 Average absolute discrepancies in the given energy intervals between the reference (ref. 10) and the incomplete basis set vibrational energy levels of H_3^+, all in cm^{-1}, computed by *different PO-DVR basis sets* using either the quadrature approximation (Appr.) or the exact-DVR (Exact) for the singular term in the Jacobi coordinate system[a]

	$(N_1\ N_2\ L) = (85\ 80\ 30)$													
	Hermite		Spherical (0,0)[b]				Spherical (0,1)[b]				Bessel			
	Appr.		Appr.		Exact		Appr.		Exact		Appr.		Exact	
Interval	Even	Odd	Even	Odd	Even	Odd	Even	Odd	Even	Odd	Even	Odd	Even	Odd
0–10 000	0.01	0.00	0.00	0.00	0.00	0.00	0.00	0.00	0.00	0.00	0.00	0.00	0.00	0.00
10 000–20 000	*49.90*	*0.29*	0.03	*2.81*	0.03	0.03	*2.31*	*3.17*	*2.32*	0.02	0.03	*3.04*	0.03	0.03
20 000–25 000	*75.89*	*1.03*	0.16	*10.39*	0.16	0.14	*3.81*	*10.83*	*3.86*	0.11	0.15	*10.40*	0.15	0.13
25 000–30 000	*74.96*	*1.46*	0.49	*16.36*	0.45	0.39	*3.36*	*15.39*	*3.49*	0.30	0.48	*14.80*	0.45	0.38
30 000–34 912	*70.79*	*1.77*	1.44	*20.10*	1.27	1.10	*2.40*	*17.47*	*2.68*	0.75	1.34	*16.73*	1.19	1.06
	$(N_1\ N_2\ L) = (95\ 90\ 35)$													
	Hermite		Spherical (0,0)[b]				Spherical (0,1)[b]				Bessel			
	Appr.		Appr.		Exact		Appr.		Exact		Appr.		Exact	
	Even	Odd	Even	Odd	Even	Odd	Even	Odd	Even	Odd	Even	Odd	Even	Odd
0–10 000	0.01	0.00	0.00	0.00	0.00	0.00	0.00	0.00	0.00	0.00	0.00	0.00	0.00	0.00
10 000–20 000	*49.85*	*0.30*	0.01	*2.53*	0.01	0.02	*2.35*	*2.60*	*2.36*	0.01	0.01	*2.49*	0.01	0.02
20 000–25 000	*75.73*	*1.05*	0.05	*8.73*	0.05	0.06	*3.97*	*9.01*	*4.01*	0.05	0.05	*8.60*	0.05	0.06
25 000–30 000	*74.56*	*1.51*	0.17	*12.63*	0.17	0.13	*3.72*	*13.04*	*3.81*	0.13	0.17	*12.44*	0.16	0.12
30 000–34 912	*69.90*	*1.92*	0.54	*14.50*	0.50	0.46	*3.14*	*15.08*	*3.32*	0.48	0.50	*14.29*	0.47	0.43

[a] All calculations were performed with $R_j^{\max} = 17.65$ bohr ($j = 1, 2$) and $m(H) = 1.007825\ u$. For Hermite-DVR $R_j^{\min} = 0.05$ bohr ($j = 1, 2$) was used. During the PO-DVR "relaxed" effective one-dimensional potentials were used, while 500 primitive basis functions were included for both stretching type coordinates. $(N_1\ N_2\ L)$ stands for using N_1, N_2, and L basis functions for the R_1, R_2, and Θ coordinates, respectively. Numbers suffering from convergence problems are indicated in italics. [b] "Spherical (n,m)" stands for spherical-oscillator-DVR radial basis sets with $\alpha = n$ and m for the R_1 and R_2 Jacobi coordinates, respectively.

more realistic barrier to linearity though the long range part was compromised. It is obviously not straightforward to find fixed values for the non-active coordinates which would provide useful PO-DVR points for the computation of the *complete* spectrum. The "relaxed" PO-DVR provides a "black-box" strategy for the determination of the PO-DVR points based on effective potentials obtained by constrained optimizations. Note that Lee and Light[38] constructed "energy selected bases" based on the same idea, *i.e.*, employing minimum-energy reduced-dimensional potentials. Fig. 2 shows that the "relaxed" potentials for H_3^+ have correct physical behaviors both at the barrier to linearity and at dissociation. Convergence of the different PO-DVRs and primitive DVRs in different spectral regions can be understood qualitatively by inspecting the distribution of the quadrature points along the coordinates for the different radial basis sets. Fig. 3 and 4 show how the PO-DVRs "optimize" the distribution of the quadrature points based on their 1D effective potentials and why the "fixed" PO-DVR only works well for low-energy vibrational states.

The failure of the quadrature approximation for odd-parity states employing PO requires further investigation. The following test computations have been carried out:

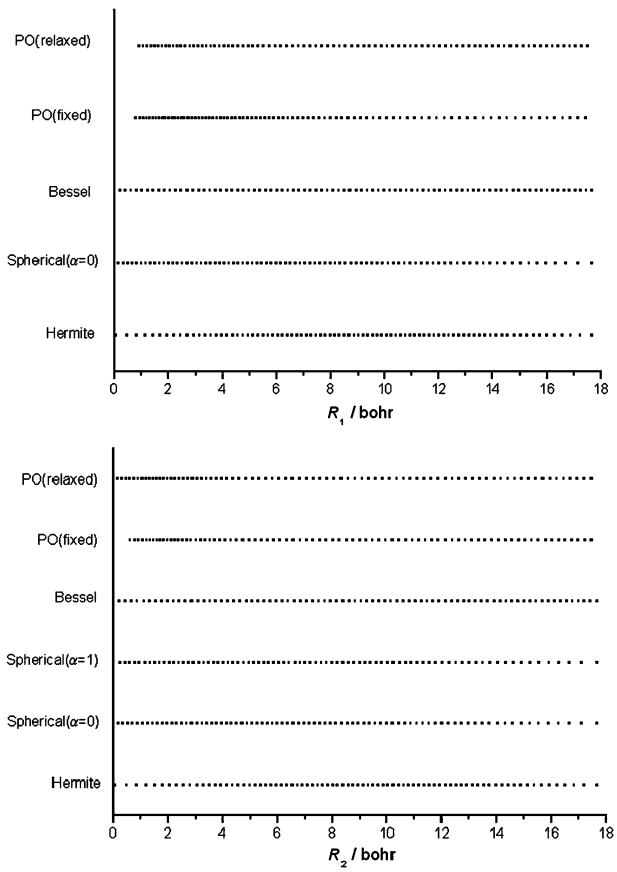

Fig. 3 Pictorial representation of the distribution of quadrature points using different DVRs with $R_1^{max} = R_2^{max} = 17.65$ bohr and setting $\ell = 0$ during PO [see eqn (20)]. Note that the PO-DVR quadrature points are numerically identical for the different primitive basis sets. 85 and 80 points are shown for the R_1 and R_2 coordinates, respectively.

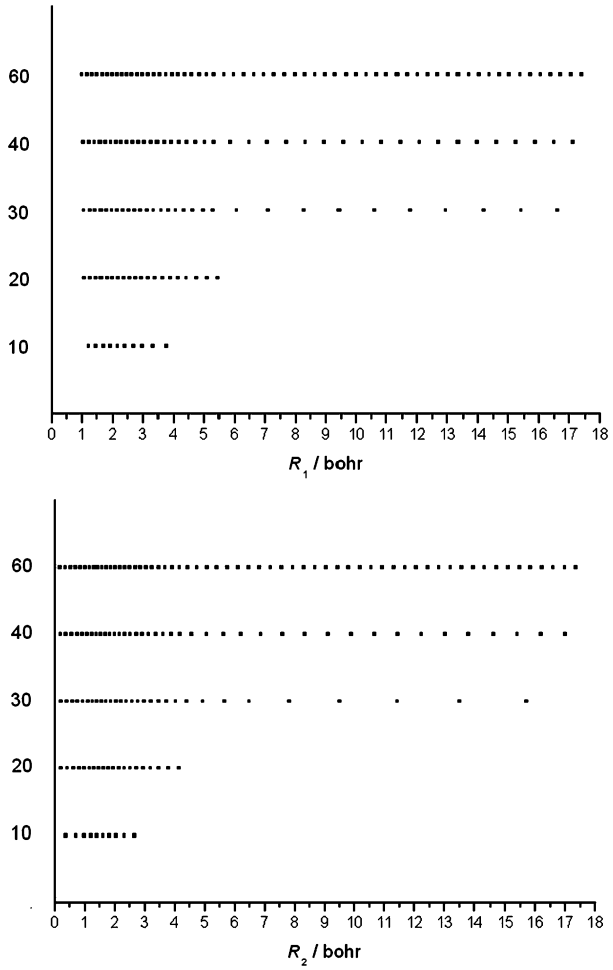

Fig. 4 Pictorial representation of different number of "relaxed" PO-DVR quadrature points with $\ell = 0$ [see eqn (20)] and keeping $R_1^{max} = R_2^{max} = 17.65$ bohr.

(a) exact-PO-DVR for R_1 and PO-DVR with quadrature approximation for R_2, (b) PO-DVR with quadrature approximation for R_1 and exact-PO-DVR for R_2, (c) PO-DVR for R_1 and primitive DVR for R_2 with quadrature approximation for both, and (d) primitive DVR for R_1 and PO-DVR for R_2 with quadrature approximation for both. These test computations showed that (a) and (d) resulted in large increases in the average errors, whereas in cases (b) and (c) the quadrature approximation did not compromise the results significantly. Thus, we verified that the failure of the PO-DVR, along with the quadrature approximation, occurs when the radial singularity comes into play (R_2 coordinate). The fact that there is no convergence problem below the barrier to linearity, see the results in the 0–10 000 cm^{-1} range in Table 4, supports this statement. It is important to note that these findings are in *partial* agreement with those of HTS,[18] who found that the quadrature approximation caused the convergence problems in their DVR3D computations using contracted DVR basis functions. The contracted basis set can be considered as PO-DVR in higher dimensions; therefore, this can be the reason of the similar convergence behavior of their computations and our odd-parity PO-DVR results. However, we cannot fully support the general statement

on the "failure of the quadrature approximation",[18] since we could compute converged odd-parity results well above the barrier to linearity using *primitive* DVR basis sets (having proper boundary conditions) with the common quadrature approximation. Furthermore, we have found that the quadrature approximation works well for all the even-parity states (see the Spherical ($\alpha = 0$) and Bessel results of Table 4).

We conclude that as long as exact-DVR is used, PO bases corresponding to relaxed 1D effective potentials seem to be the best choice with the fastest convergence (up to about 1 cm^{-1} for levels near the dissociation limit) and resulting in the "complete" (see section VI.3) set of eigenvalues even in the uppermost region of the spectrum. Besides giving the best numerical results, there are some other benefits of using PO-DVR. Compared to the corresponding primitive basis, results are less sensitive to the parameters R_j^{max}, as long as they are large enough for the 1D effective potentials to reach their asymptotic region. Another benefit is that the results are invariant to the actual form of the primitive basis as long as it has proper boundary conditions and convergence is attained for the 1D problem, *i.e.* eqn (20), since in this case the 1D eigenfunctions (the PO radial basis functions) are numerically the same for different primitive basis sets.

VI.3 Near-dissociation vibrational levels of H_3^+

In Table 5 we present the highest 15 even-parity and 15 odd-parity vibrational levels just below D_0 and their dependence on basis set size and the parameters R_j^{max} ($j = 1$ or 2), obtained by "relaxed" PO exact Bessel-DVR. The complete list of our benchmark-quality bound vibrational energy levels corresponding to the PPKT2 PES of ref. 10 is given in Table S2 in the ESI.† The largest computation employed $120 \times 120 \times 51 = 734\,400$ basis functions for each block (even and odd). All computed energy levels near dissociation are converged to at least about 1 cm^{-1}. The rate of convergence is visually demonstrated in Fig. 5. To achieve convergence for diffuse vibrational states near dissociation the R_j^{max} ($j = 1$ or 2) parameters were set to 22 bohr (17.65 bohr was used for Tables 3 and 4), although this causes the less diffuse lower energy states to be less converged. We have found 688 even and 599 odd parity vibrational band origins below D_0. The calculated eigenenergies are in good agreement with the results presented by Munro *et al.*,[10] except at the very top end of the spectrum. For the even-parity block one additional eigenstate was found, and deviations larger than 1 cm^{-1}, *i.e.* 1–6 cm^{-1}, can also be seen among the last 4 and 3 band origins for the even and odd blocks, respectively. Using $R_j^{max} = 17.65$ bohr

Table 5 Convergence of near-dissociation vibrational band origins of H_3^+ with respect to basis set size and the parameters R_j^{max}($j = 1$ or 2). Results are calculated in Jacobi coordinates employing PO(relaxed) exact Bessel-DVR, deviations and band origins are all given in cm^{-1}[a]

R_j^{max}	17.65	19.00	20.00	21.00	22.00	22.00					
Basis[b]	(115 110 38)					(105 100 38)	(115 110 38)	(120 120 45)	(120 120 48)	(120 120 51)	Ref. 10
Even											
674	0.14	0.23	0.01	−0.02	34769.05	−0.38	−0.05	0.00	0.00	34769.10	34769.66
675	−0.13	0.09	0.11	0.08	34790.26	−0.26	0.00	0.00	0.00	34790.27	34790.86
676	0.24	0.04	0.07	0.16	34794.41	0.72	−0.26	0.00	0.00	34794.67	34795.46
677	−0.18	0.02	−0.05	−0.11	34811.31	−0.34	0.09	0.00	0.00	34811.22	34811.71
678	0.13	0.25	0.01	−0.02	34823.28	0.37	0.02	0.00	0.00	34823.26	34823.96
679	−0.18	−0.08	−0.05	0.00	34824.61	−0.33	0.02	0.00	0.00	34824.59	34825.22
680	−0.16	−0.10	−0.18	−0.10	34835.91	0.11	0.17	0.00	0.00	34835.74	34836.53
681	−0.07	0.27	0.09	−0.16	34851.58	−0.20	0.12	0.00	0.00	34851.46	34852.01
682	−0.05	−0.33	−0.61	−0.45	34857.66	0.24	0.47	0.00	0.00	34857.18	34858.11
683	−0.04	0.10	0.01	−0.03	34864.91	0.39	0.02	0.00	0.00	34864.89	34865.42
684	−0.25	0.17	0.10	0.07	34882.36	−0.57	0.00	0.00	0.00	34882.35	34882.98
685	0.99	0.59	0.18	−0.02	34889.16	−0.63	−0.67	−0.02	0.00	34889.83	34891.35
686	1.78	2.00	1.36	0.35	34895.71	−1.26	−1.34	0.00	0.00	34897.06	34898.00
687	3.10	2.11	0.53	0.06	34896.97	−1.11	−2.08	−0.06	0.00	34899.05	34901.02
688	13.45	9.00	1.78	0.28	34901.31	−9.58	−9.65	−1.76	0.05	34910.96	—
Odd											
585	0.13	0.30	0.27	0.29	34743.53	−0.80	−0.21	0.00	0.00	34743.74	34744.51
586	0.18	0.24	0.09	0.02	34750.04	−0.56	−0.06	0.00	0.00	34750.10	34751.21
587	−2.88	−1.38	−0.01	0.43	34763.40	−2.73	−0.51	0.00	0.00	34763.91	34762.54
588	−0.66	−0.50	−0.37	−0.34	34790.70	−0.59	0.14	0.00	0.00	34790.57	34790.82
589	0.45	0.65	0.43	0.24	34794.30	−0.71	−0.18	0.00	0.00	34794.49	34795.42
590	−0.37	0.01	0.04	0.07	34808.25	−0.39	−0.09	0.00	0.00	34808.34	34808.46
591	−0.36	0.22	0.31	0.09	34811.46	−1.34	−0.23	0.00	0.00	34811.69	34812.02
592	−0.66	0.13	0.43	0.40	34823.58	−1.33	−0.26	0.00	0.00	34823.84	34823.93
593	−0.36	−0.15	0.05	0.28	34834.17	−0.83	−0.05	0.00	0.00	34834.22	34834.89
594	0.55	0.62	0.40	0.23	34835.34	0.35	−0.20	0.00	0.00	34835.54	34836.45
595	0.00	0.88	0.91	0.60	34857.27	−1.43	−0.47	0.00	0.00	34857.73	34857.93
596	0.30	0.64	0.58	0.41	34864.53	−0.69	−0.38	0.00	0.00	34864.91	34865.37
597	0.61	0.47	0.23	0.11	34881.86	0.40	−0.09	0.00	0.00	34881.94	34882.98
598	2.92	3.03	1.94	0.40	34893.64	−2.71	−2.72	0.00	0.00	34896.36	34897.10
599	3.75	1.99	0.13	0.28	34896.41	−3.15	−2.56	−0.18	−0.01	34898.97	34904.62

[a] The same PES and masses, *i.e.* $m(H) = 1.007825\ u$, have been employed in ref. 10 and in this study. [b] During the PO-DVR 600 primitive Bessel-DVR basis functions were used for both stretching type coordinates. (N_1 N_2 L) stands for using N_1, N_2, and L basis functions for the R_1, R_2, and Θ coordinates, respectively. Note that L stands for L basis functions for one symmetry block only, meaning $2 \times L$ basis functions altogether.

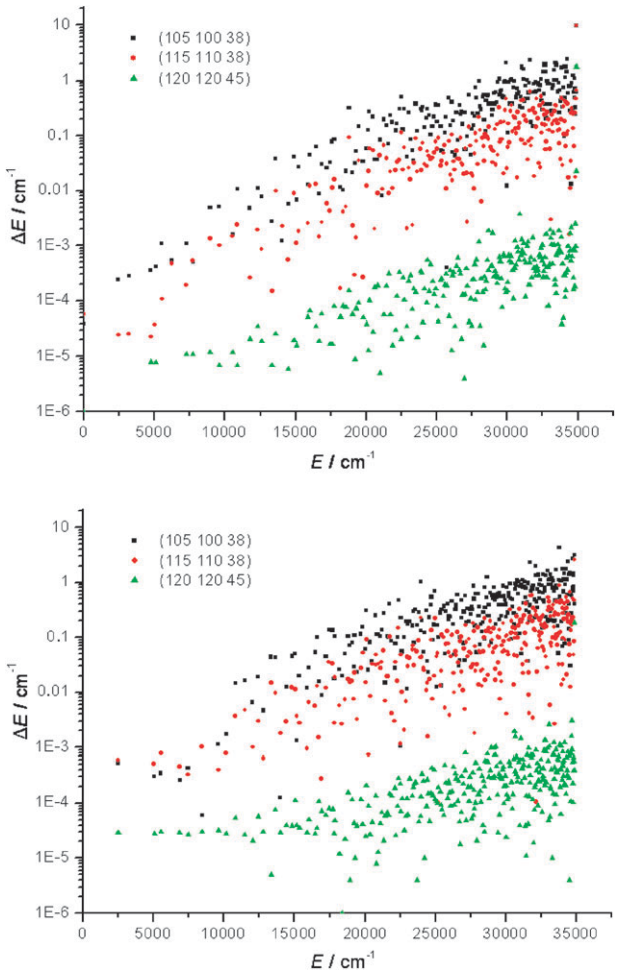

Fig. 5 Pictorial demonstration of the convergence rate for even (upper panel) and odd (lower panel) parity states of H_3^+ computed by the method of "relaxed" PO exact Bessel-DVR. (N_1 N_2 L) stands for using N_1, N_2, and L basis functions for the R_1, R_2, and Θ coordinates, respectively. Absolute deviations from the energies obtained with the (120 120 51) basis are shown on a logarithmic scale.

we also obtained only 687 even and 599 odd bound states as in ref. 10. The increase of the largest grid points up to 19–20 bohr resulted in the appearance of an additional even-parity level below D_0 and $R_j^{\max}$ had to be increased up to 22 bohr in order to get this new asymptotic vibrational state converged to within 1 cm^{-1}. The presence of further near dissociation eigenstates was predicted in ref. 10. We have found one, but additional highly diffuse states may exist.

VII. Summary and conclusions

Several techniques were investigated in order to develop a highly efficient algorithm for the solution of the time-independent vibrational Schrödinger equation. The algorithms investigated allow the computation of complete (ro)vibrational spectra of triatomic molecules, using *orthogonal* internal coordinates of the two distance–one angle type. Effectiveness of the possible protocols was judged by their ability to properly treat the singularities present in the kinetic energy operator and by the associated computational cost. The representations D^3OPI, ED^3OPI, D^2FOPI and ED^2FOPI were introduced, based on the use of a direct-product basis built from one-dimensional discrete variable representation (DVR) bases corresponding to the two distance-type coordinates and orthogonal Legendre polynomials, or the corresponding Legendre-DVR basis, corresponding to the angular coordinate. The efficient analytical treatment of the angular singularity is ensured by the use of Legendre functions, eigenfunctions of the angular part of the kinetic energy operator. For the treatment of the radial singularity the use of (a) DVRs employing the quadrature approximation and (b) special DVRs satisfying the boundary conditions and thus allowing for the use of exact DVR expressions were considered. Effects of basis set boundary conditions were also thoroughly studied. In order to obtain more compact radial basis sets, potential optimized (PO) DVRs, based on one-dimensional Hamiltonians with potentials obtained by (a) fixing (in the present case at the equilibrium) or (b) relaxing the two non-active coordinates, were also considered. Calculations employed Hermite-DVR, spherical-oscillator-DVRs, and Bessel-DVR bases as primitive radial functions. A new analytical formula was given for the determination of the matrix elements of the singular R^{-2} operator using a certain Bessel-DVR developed by Littlejohn and Cargo.[25] The utility of the different algorithms were demonstrated by the computation of converged near-dissociation vibrational energy levels of the H_3^+ molecular ion.

The most important numerical results of the present study are summarized as follows:

(1) If one were to compute (ro)vibrational energy levels with wave functions having a finite amplitude at the boundary, basis sets with proper boundary conditions need to be used.

(2) In the case of primitive DVRs either the quadrature approximation or exact-DVR can be applied for the evaluation of the singular terms, even when the wave function does not vanish at the singular nuclear geometries. This statement is in contrast to the usually claimed failure of the quadrature approximation in certain singular integrals. This general result can be of great help to reduce the cost of computations limited by computer power, such as (ro)vibrational calculations on four- or five-atomic molecules.

(3) The use of exact-DVR shows faster convergence; thus, if the quadrature approximation does not result in major computational benefits, the exact-DVR is recommended. When considering such decisions, sequential summation (see section III) should also be taken into account, since it might significantly decrease the overall computational cost.

(4) The numerical results also show that using PO-DVRs might be necessary to optimize the quadrature points for calculations with larger coordinate ranges, where the number of primitive basis functions needed for obtaining converged results would become unaffordable. This was the case for the computation of some extremely diffuse near dissociation eigenstates of H_3^+ in the present study. Despite their many useful properties, see section VI.2, it is emphasized that PO-DVRs should be constructed with great caution and employing relaxed 1D effective potentials.

(5) For computing the near dissociation vibrational levels of H_3^+ corresponding to the electronic ground state, the use

of the ED^{2}FOPI (see section II.4) representation (thus exact-DVR) employing "relaxed" PO-DVR constructed from either Bessel-DVR or spherical-oscillator-DVR (with $\alpha = 0$ for both R_1 and R_2 coordinates) seems to be the best choice. With this method, all the 1287 (counting the E-symmetry states twice) bound vibrational energy levels of the H_3^+ molecule could be calculated in a few days on a single processor personal computer with a convergence of at least about 1 cm^{-1}.

Finally, although the present study considers only vibrations, it is important to address singularities related to the rotational motion, as well. The form of the rovibrational Hamiltonian depends on the choice of the embedding; for example, there exist R_1-, R_2-, bisector, and z-perpendicular embeddings.[1,3] In all cases further singular terms appear in the Hamiltonian. Among these new terms one always finds the terms R_1^{-2} or R_2^{-2}, or both, where the conclusions of the present study, *i.e.*, the performance of the quadrature approximation *vs.* the exact DVR, are directly useful. In certain embeddings additional angular singularities may arise, which may require further considerations.

Acknowledgements

The work performed has been supported by the Hungarian Scientific Research Fund, OTKA, through grant K72885. Discussions with Dr Edit Mátyus and Mr Csaba Fábri are gratefully acknowledged.

References

1 B. T. Sutcliffe and J. Tennyson, *Int. J. Quantum Chem.*, 1991, **39**, 183.
2 (*a*) D. W. Schwenke, *Comput. Phys. Commun.*, 1992, **70**, 1; (*b*) N. E. Klepeis, A. L. L. East, A. G. Császár, W. D. Allen, T. J. Lee and D. W. Schwenke, *J. Chem. Phys.*, 1993, **99**, 3865.
3 (*a*) J. R. Henderson and J. Tennyson, *Comput. Phys. Commun.*, 1993, **75**, 365; (*b*) J. Tennyson, J. R. Henderson and N. G. Fulton, *Comput. Phys. Commun.*, 1995, **86**, 175.
4 (*a*) G. Czakó, T. Furtenbacher, A. G. Császár and V. Szalay, *Mol. Phys.*, 2004, **102**, 2411; (*b*) T. Furtenbacher, G. Czakó, B. T. Sutcliffe, A. G. Császár and V. Szalay, *J. Mol. Struct.*, 2006, **780–781**, 283.
5 M. Mladenović, *J. Chem. Phys.*, 2000, **112**, 1070.
6 M. J. Bramley and T. Carrington Jr., *J. Chem. Phys.*, 1993, **99**, 8519.
7 S. Carter and N. C. Handy, *Comput. Phys. Rep.*, 1986, **5**, 117.
8 H.-S. Lee and J. C. Light, *J. Chem. Phys.*, 2004, **120**, 4626.
9 J. Tennyson, P. Barletta, J. J. Munro and B. C. Silva, *Philos. Trans. R. Soc. London, Ser. A*, 2006, **364**, 2903.
10 J. J. Munro, J. Ramanlal, J. Tennyson and H. Y. Mussa, *Mol. Phys.*, 2006, **104**, 115.
11 E. Mátyus, G. Czakó, B. T. Sutcliffe and A. G. Császár, *J. Chem. Phys.*, 2007, **127**, 084102.
12 S. Carter, J. M. Bowman and N. C. Handy, *Theor. Chem. Acc.*, 1998, **100**, 191.
13 (*a*) C. Eckart, *Phys. Rev.*, 1935, **47**, 552; (*b*) J. K. G. Watson, *Mol. Phys.*, 1968, **15**, 479.
14 E. Mátyus, G. Czakó and A. G. Császár, *J. Chem. Phys.*, 2009, **130**, 134112.
15 D. Luckhaus, *J. Chem. Phys.*, 2000, **113**, 1329.
16 D. Lauvergnat and A. Nauts, *J. Chem. Phys.*, 2002, **116**, 8560.
17 S. N. Yurchenko, W. Thiel and P. Jensen, *J. Mol. Spectrosc.*, 2007, **245**, 126.
18 J. R. Henderson, J. Tennyson and B. T. Sutcliffe, *J. Chem. Phys.*, 1993, **98**, 7191.
19 S. Carter and W. Meyer, *J. Chem. Phys.*, 1992, **96**, 2424.
20 J. K. G. Watson, *Chem. Phys.*, 1995, **190**, 291.
21 B. R. Johnson, *J. Chem. Phys.*, 1980, **73**, 5051.
22 M. J. Bramley, J. W. Tromp, T. Carrington Jr. and G. C. Corey, *J. Chem. Phys.*, 1994, **100**, 6175.
23 G. Czakó, V. Szalay, A. G. Császár and T. Furtenbacher, *J. Chem. Phys.*, 2005, **122**, 024101.
24 R. G. Littlejohn, M. Cargo, T. Carrington Jr., K. A. Mitchell and B. Poirier, *J. Chem. Phys.*, 2002, **116**, 8691.
25 R. G. Littlejohn and M. Cargo, *J. Chem. Phys.*, 2002, **117**, 27.
26 G. Czakó, V. Szalay and A. G. Császár, *J. Chem. Phys.*, 2006, **124**, 014110.
27 G. Czakó, T. Furtenbacher, P. Barletta, A. G. Császár, V. Szalay and B. T. Sutcliffe, *Phys. Chem. Chem. Phys.*, 2007, **9**, 3407.
28 C. G. J. Jacobi, *Cr. Hebd. Acad. Sci.*, 1842, **15**, 236.
29 R. Radau, *Ann. Sci. Ecole Norm. S*, 1868, **5**, 311.
30 V. Szalay, *J. Chem. Phys.*, 1993, **99**, 1978.
31 D. O. Harris, G. G. Engerholm and W. D. Gwinn, *J. Chem. Phys.*, 1965, **43**, 1515.
32 J. Tennyson and B. T. Sutcliffe, *J. Mol. Spectrosc.*, 1983, **101**, 71.
33 J. Echave and D. C. Clary, *Chem. Phys. Lett.*, 1992, **190**, 225.
34 H. Wei and T. Carrington Jr., *J. Chem. Phys.*, 1992, **97**, 3029.
35 V. Szalay, G. Czakó, Á. Nagy, T. Furtenbacher and A. G. Császár, *J. Chem. Phys.*, 2003, **119**, 10512.
36 O. L. Polyansky, R. Prosmiti, W. Klopper and J. Tennyson, *Mol. Phys.*, 2000, **98**, 261.
37 J. J. Munro, J. Ramanlal and J. Tennyson, *New J. Phys.*, 2005, **7**, 196.
38 H.-S. Lee and J. C. Light, *J. Chem. Phys.*, 2003, **118**, 3458.

